

Synthesis of Quinoxaline-Based Donor–Acceptor Narrow-Band-Gap Polymers and Their Cyclized Derivatives for Bulk-Heterojunction Polymer Solar Cell Applications

Jie Zhang, Wanzhu Cai, Fei Huang,* Ergang Wang, Chengmei Zhong, Shengjian Liu, Ming Wang, Chunhui Duan, Tingbin Yang, and Yong Cao*

Institute of Polymer Optoelectronic Materials & Devices, Key Laboratory of Specially Functional Materials of the Ministry of Education, South China University of Technology, Guangzhou 510640, P. R. China

Received November 30, 2010; Revised Manuscript Received January 14, 2011

ABSTRACT: A series of narrow-band-gap donor–acceptor (D–A) conjugated polymers, with thiophene-substituted quinoxaline monomer 5,8-bis(5-bromothiophen-2-yl)-2,3-bis(5-octylthiophen-2-yl)quinoxaline (TTQx) or its cyclized phenazine derivative monomer 8,11-bis(5-bromothiophen-2-yl)-2,5-diocetylthienopyrazine [2,3-*a*:3',2'-*c*]phenazine (TTPz) as acceptors, were synthesized via Suzuki coupling reaction. It was found that the copolymers based on thiophene-substituted quinoxaline TTQx exhibit obviously red-shifted absorbance compared to previously reported D–A copolymers based on phenyl-substituted quinoxaline. Their analogous copolymers based on the cyclized TTPz acceptor show more pronounced red-shifted absorption spectra with a significantly decreased band gap due to the enlarged planar polycyclic aromatic ring of TTPz. Moreover, compared to the copolymers based on TTQx, the TTPz-based copolymers' mobilities are also significantly increased due to the reduced steric hindrance and improved structural planarity among the copolymers. Bulk-heterojunction polymer solar cells based on the blends of the copolymers with a fullerene derivative as an acceptor exhibit promising performance, and the best device performance with power conversion efficiency up to 4.4% was achieved.

Introduction

In the past decade, polymer solar cells (PSCs) have attracted considerable attention for their unique advantages over traditional silicon-based solar cells, such as low cost, light weight, and the potential for making flexible large area devices by roll-to-roll manufacturing.^{1–7} Most of PSCs use a bulk-heterojunction-type (BHJ) device structure with a phase-separated blend of organic electron donor and acceptor components as active layer, where an electron-donating conjugated polymer and an electron-accepting fullerene derivative, such as (6,6)-phenyl-C₆₁-butyric acid methyl ester (PC₆₁BM) or (6,6)-phenyl-C₇₁-butyric acid methyl ester (PC₇₁BM), are commonly used as donor and acceptor, respectively.^{1,8}

To achieve high-performance BHJ type PSCs, the electron-donating conjugated polymers need to have strong and broad absorption for the solar light, a good hole mobility, and reasonable highest occupied molecular orbital levels (HOMO) to maximize the short-circuit current (J_{sc}) and open-circuit voltage (V_{oc}), respectively. Poly(3-hexylthiophene) (P3HT) is one of the most promising donor materials, and the power conversion efficiency (PCE) of PSCs based on its thin film blend with PC₆₁BM has often reached ~4–5%.^{9–11} However, P3HT's absorption does not match well with the solar spectrum, and its HOMO (~–5.0 eV) is relative high which limits the magnitude of the J_{sc} and V_{oc} , respectively. Thus, it is difficult to further improve the efficiency of P3HT-based PSCs,¹² except for using new fullerene derivative acceptors.^{13,14} To overcome this, one feasible approach is to design alternating donor–acceptor (D–A) copolymers combined electron-rich unit (donor) and electron-deficient unit (acceptor),

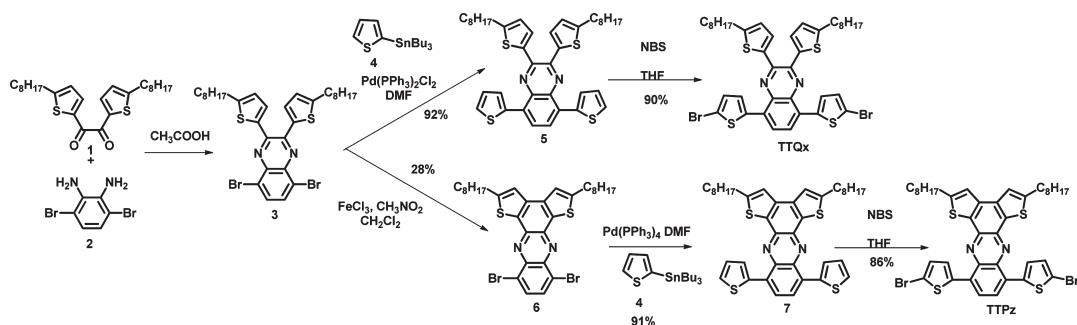
where the absorption and energy level of the copolymers can be readily tuned by controlling the intermolecular charge transfer from the donor to the acceptor. Recently, many kinds of D–A copolymers have been successfully developed and show excellent photovoltaic properties with PCE as high as ~3–7% by choosing various electron donors (such as fluorene, carbazole, or silafluorene, etc.) and acceptors (such as benzothiadiazole, quinoxaline, or thieno[3,4-*c*]pyrrole-4,6-dione, etc.).^{15–38}

Among them, quinoxaline-based D–A copolymers have been successfully developed and exhibit promising photovoltaic performance due to that the electron-deficient N-heterocycle of quinoxaline can effectively tune the energy level and lower the band gap of the resulting copolymers.^{18,32–38} For example, poly[2,7-(9,9-dioctylfluorene)-*alt*-5,5-(5',8'-di-2-thienyl)-(2',3'-bis(3''-octyloxyphenyl)quinoxaline)] (APFO-15) possessed a very low-lying HOMO of –5.36 eV, a high V_{oc} of 1.0 V, and a PCE of 3.5%.^{18,32} By using PC₇₁BM as the acceptor, another kind of quinoxaline-based D–A copolymer poly[2,3-bis(3-octyloxyphenyl)quinoxaline-5,8-diyl-*alt*-thiophene-2,5-diyl] (TQ1) exhibited a high PCE of 6.0% with a V_{oc} of ~0.9 V.³⁵ Despite of their promising device performance, most of the currently reported quinoxaline-based D–A copolymers contain two pendant substituted benzene groups on the quinoxaline rings, which can freely rotate and potentially hinder the intermolecular packing of the copolymers and further influence their mobility. Thus, if the two pendant substituted aromatic rings can be replaced by an enlarged fused planar aromatic ring, the π – π interaction among the resulted copolymers will be enhanced and the mobility will be improved, which is favorable for PSCs application.^{39–41}

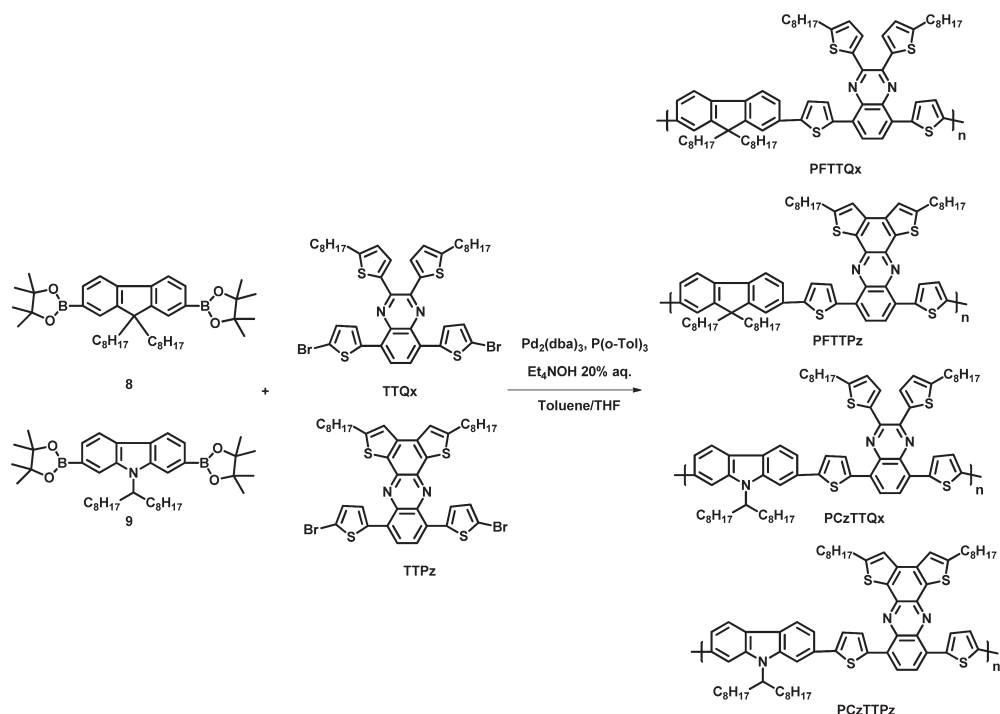
In this work, a series of new quinoxaline-based D–A copolymers poly[2,7-(9,9-dioctylfluorene)-*alt*-5,5-(5',8'-di-2-thienyl)-(2',3'-bis(5''-octylthiophen-2''-yl)quinoxaline)] (PFTTQx),

*Corresponding authors. E-mail: msfhuang@scut.edu.cn (F.H.); yongcao@scut.edu.cn (Y.C.).

Scheme 1. Synthesis of the Monomers



Scheme 2. Synthesis of the Copolymers



poly[2,7-(9,9-dioctylfluorene)-*alt*-5,5-(8',11'-di-2-thinenyl)-(2',5'-dioctyldithieno[2',3'-*a*:3'',2''-*c*]phenazine)] (PFTTPz), poly[*N*-9'-heptadecanyl-2,7-cabazole-*alt*-5,5-(5',8'-di-2-thinenyl)-(2',3'-bis(5''-octylthiophen-2''-yl)quinoxaline)] (PCzTTQx), and poly[*N*-9'-heptadecanyl-2,7-cabazole-*alt*-5,5-(8',11'-di-2-thinenyl)-(2',5'-dioctyldithieno[2',3'-*a*:3'',2''-*c*]phenazine)] (PCzTTPz) were synthesized via Suzuki coupling reaction (Schemes 1 and 2). Compared to previously reported benzene-substituted quinoxaline copolymers, the copolymers based on thiophene-substituted quinoxaline acceptors PFTTQx and PCzTTQx exhibit red-shifted absorption with a band gap of 1.86 and 1.90 eV, respectively. Moreover, the two pendant substituted thiophene rings of PFTTQx and PCzTTQx could be easily oxidize cyclized to form an enlarged planar polycyclic aromatic ring. The resulted D–A copolymers based on the polycyclic aromatic ring PFTTPz and PCzTTPz show significantly red-shifted absorption with a smaller band gap of 1.68 and 1.66 eV, respectively, and higher mobility than those of the copolymers PFTTQx and PCzTTQx. Photovoltaic properties of these copolymers were investigated. Overall efficiencies over 2% are achieved for the PSCs based on the blend active layer of the copolymers and PC₇₁BM. Among them, PFTTQx showed the best performance with a PCE of 4.4%, a V_{oc} of 0.90 V, a J_{sc} of 7.4 mA cm⁻², and a fill factor (FF) of 0.59.

Experimental Section

Materials. 1,2-Bis(5-octylthiophen-2-yl)ethane-1,2-dione (**1**),⁴² 3,6-dibromobenzene-1,2-diamine (**2**),¹⁸ 2,7-bis(4,4,5,5-tetramethyl-1,3,2-dioxaborolan-2-yl)-9,9-dioctylfluorene (**8**),²⁰ and 2,7-bis-(4',4',5',5'-tetramethyl-1',3',2'-dioxaborolan-2'-yl)-*N*-9'-heptadecanylethylcarbazole (**9**)²² were prepared according to the reported procedures. All chemicals and reagents were purchased from commercial sources (Aldrich, Acros, and Alfa Aesar) and used without further purification unless stated otherwise.

5,8-Dibromo-2,3-bis(5-octylthiophen-2-yl)quinoxaline (3). A mixture of 1,2-bis(5-octylthiophen-2-yl)ethane-1,2-dione (**1**) (4.46 g, 10.0 mmol), 3,6-dibromobenzene-1,2-diamine (**2**) (3.20 g, 12.0 mmol), and acetic acid (70 mL) was stirred at 40 °C for 10 h and then was poured into brine. It was then extracted with dichloromethane, the two phases were separated, and the water phase was extracted twice with dichloromethane. The combined organic extracts were washed three times with water, dried over magnesium sulfate, evaporated, and purified with column chromatography (silica gel, petroleum ether/dichloromethane (5/1) as eluent) to yield 6.15 g (91%) of **3** as a yellowish solid. ¹H NMR (CDCl₃, 300 MHz) δ (ppm): 7.76 (s, 2H), 7.40 (d, J = 3.6 Hz, 2H), 6.71 (d, J = 3.6 Hz, 2H), 2.86 (t, J = 7.8 Hz, 4H), 1.77–1.69 (m, 4H), 1.43–1.25 (m, 20H), 0.88 (t, J = 6.9 Hz, 6H). ¹³C NMR (CDCl₃, 75 MHz) δ (ppm): 152.1, 147.2, 138.5, 138.3, 132.6, 130.4,

125.0, 122.9, 31.9, 31.5, 30.5, 29.3, 29.2, 29.1, 22.7, 14.1. MS (APCI): calcd 676.6, found $(M + 1)^+$ 677.6. Anal. Calcd for $C_{32}H_{40}Br_2N_2S_2$ (%): C 56.80, H 5.96, N 4.14, S 9.48. Found (%): C 56.38, H 6.32, N 4.15, S 10.34.

2,3-Bis(5-octylthiophen-2-yl)-5,8-di(thiophen-2-yl)quinoxaline (5). $PdCl_2(PPh_3)_2$ (28 mg, 0.024 mmol) was added to a solution of compound **3** (1.35 g, 2 mmol) and 2-(tributylstannyl)-thiophene (**4**) (1.57 g, 4.2 mmol) in 50 mL of dimethylformamide (DMF). The mixture was heated at 110 °C in a nitrogen atmosphere overnight. The reaction was quenched with aqueous $NaHCO_3$ and extracted with dichloromethane. The two phases were separated, and the water phase was extracted twice with dichloromethane. The combined organic extracts were washed three times with water, dried over magnesium sulfate, evaporated, and purified with column chromatography (silica gel, petroleum ether/dichloromethane (6/1) as eluent) to yield 1.26 g (92%) of **5** as a yellow solid. 1H NMR ($CDCl_3$, 300 MHz) δ (ppm): 8.00 (s, 2H), 7.86 (dd, $J = 1.2, 3.9$ Hz, 2H), 7.51 (dd, $J = 1.2, 5.1$ Hz, 2H), 7.40 (d, $J = 3.6$ Hz, 2H), 7.18 (dd, $J = 3.9, 5.1$ Hz, 2H), 6.70 (d, $J = 3.6$ Hz, 2H), 2.88 (t, $J = 7.7$ Hz, 4H), 1.80–1.70 (m, 4H), 1.43–1.29 (m, 20H), 0.91 (t, $J = 6.9$ Hz, 6H). ^{13}C NMR ($CDCl_3$, 75 MHz) δ (ppm): 150.9, 144.9, 139.2, 138.9, 136.4, 130.7, 130.0, 128.4, 126.9, 126.8, 126.7, 124.7, 31.9, 31.5, 30.4, 29.3, 29.2, 29.1, 22.7, 14.1. MS (APCI): calcd 680.1, found $(M + 1)^+$ 681.1. Anal. Calcd for $C_{40}H_{46}N_2S_4$ (%): C 70.33, H 6.79, N 4.10, S 18.78. Found (%): C 69.85, H 6.74, N 4.14, S 19.39.

5,8-Bis(5-bromothiophen-2-yl)-2,3-bis(5-octylthiophen-2-yl)-quinoxaline (TTQx). Compound **5** (1.26 g, 1.85 mmol) was dissolved in 30 mL of tetrahydrofuran (THF), and then *N*-bromosuccinimide (NBS) (0.73 g, 4.1 mmol) was added in portions. The mixture was heated at 40 °C for 3 h. Then the mixture was poured into brine and extracted twice with dichloromethane. The combined organic layers were dried over magnesium sulfate, and the solvent was removed. The crude product was purified with column chromatography (silica gel, petroleum ether/dichloromethane (6/1) as eluent) to yield 1.43 g (90%) of TTQx as an orange-yellow solid. 1H NMR ($CDCl_3$, 300 MHz) δ (ppm): 7.82 (s, 2H), 7.46 (d, $J = 3.9$ Hz, 2H), 7.37 (d, $J = 3.6$ Hz, 2H), 7.07 (d, $J = 3.9$ Hz, 2H), 6.71 (d, $J = 3.6$ Hz, 2H), 2.90 (t, $J = 7.7$ Hz, 4H), 1.85–1.73 (m, 4H), 1.45–1.25 (m, 20H), 0.89 (t, $J = 6.9$ Hz, 6H). ^{13}C NMR ($CDCl_3$, 75 MHz) δ (ppm): 151.4, 145.2, 139.7, 138.7, 135.8, 130.3, 129.9, 129.2, 125.8, 125.5, 124.7, 116.6, 31.9, 31.5, 30.4, 29.3, 29.1, 22.7, 14.1. MS (APCI): calcd 840.8, found $(M + 1)^+$ 841.8. Anal. Calcd for $C_{40}H_{44}Br_2N_2S_4$ (%): C 57.14, H 5.27, N 3.33, S 15.25. Found (%): C 58.15, H 5.65, N 3.33, S 14.93.

8,11-Dibromo-2,5-diethylthiopheno[2,3-*a*:3',2'-*c*]phenazine (6). To a solution of compound **3** (2.02 g, 3 mmol) in 75 mL of dry dichloromethane was added a solution of $FeCl_3$ (6.0 g, 36.9 mmol) in CH_3NO_2 (40 mL) at reflux. After 24 h, 80 mL of anhydride methanol was added to quench the reaction. It was then extracted with dichloromethane, the two phases were separated, and the water phase was extracted twice with dichloromethane. The combined organic extracts were washed three times with water, dried over magnesium sulfate, evaporated, and purified with column chromatography (silica gel, petroleum ether/dichloromethane (7/1) as eluent) to yield 0.57 g (28%) of **6** as red solid. 1H NMR ($CDCl_3$, 300 MHz) δ (ppm): 7.93 (s, 2H), 7.30 (s, 2H), 3.03 (t, $J = 7.7$ Hz, 4H), 1.89–1.79 (m, 4H), 1.45–1.29 (m, 20H), 0.89 (t, $J = 6.9$ Hz, 6H). ^{13}C NMR ($CDCl_3$, 75 MHz) δ (ppm): 153.7, 139.8, 139.1, 137.9, 132.5, 131.9, 123.4, 120.3, 31.9, 31.5, 31.2, 29.4, 29.2, 29.1, 22.7, 14.1. MS (APCI): calcd 674.6, found $(M + 1)^+$ 675.6. Anal. Calcd for $C_{32}H_{38}Br_2N_2S_2$ (%): C 56.97, H 5.68, N 4.15, S 9.51. Found (%): C 54.91, H 5.84, N 3.81, S 9.54.

2,5-Dioctyl-8,11-di(thiophen-2-yl)dithieno[2,3-*a*:3',2'-*c*]phenazine (7). $Pd(PPh_3)_4$ (46.2 mg, 0.04 mmol) was added to a solution of compound **6** (1.35 g, 2 mmol) and compound **4** (1.57 g, 4.2 mmol) in 50 mL of DMF. The mixture was heated at 110 °C

in a nitrogen atmosphere overnight. The reaction was quenched with aqueous $NaHCO_3$ extracted with dichloromethane, the two phases were separated, and the water phase was extracted twice with dichloromethane. The combined organic extracts were washed three times with water and dried over magnesium sulfate. After removal of the solvent, the residue was purified with column chromatography (silica gel, petroleum ether/dichloromethane (4/1) as eluent) to yield 1.24 g (91%) of **7** as a red solid. 1H NMR ($CDCl_3$, 300 MHz) δ (ppm): 8.19 (s, 2H), 7.96 (dd, $J = 1.0, 3.7$ Hz, 2H), 7.60 (dd, $J = 1.0, 5.1$ Hz, 2H), 7.36 (s, 2H), 7.23 (dd, $J = 3.7, 5.1$ Hz, 2H), 3.03 (t, $J = 7.6$ Hz, 4H), 1.91–1.81 (m, 4H), 1.54–1.30 (m, 20H), 0.89 (t, $J = 6.9$ Hz, 6H). ^{13}C NMR ($CDCl_3$, 75 MHz) δ (ppm): 152.5, 139.1, 137.6, 137.5, 137.1, 133.2, 130.8, 128.9, 126.3, 126.0, 125.7, 120.0, 31.9, 31.5, 31.1, 29.4, 29.3, 22.7, 14.1. MS (APCI): calcd 681.0, found $(M)^+$ 681.4. Anal. Calcd for $C_{40}H_{44}N_2S_4$ (%): C 70.54, H 6.51, N 4.11, S 18.83. Found (%): C 70.40, H 6.53, N 4.09, S 18.94.

8,11-Bis(5-bromothiophen-2-yl)-2,5-diethylthiopheno[2,3-*a*:3',2'-*c*]phenazine (TTPz). Compound **7** (0.68 g, 1.0 mmol) was dissolved in 200 mL of THF, and then NBS (0.374 g, 2.1 mmol) was added in portions. The mixture was heated at 40 °C for 3 h. Then the mixture was poured into brine and extracted twice with dichloromethane. The combined organic layers were dried over magnesium sulfate, and the solvent was removed. The crude product was purified with column chromatography (silica gel, petroleum ether/dichloromethane (6/1) as eluent) to yield 0.72 g (86%) of TTPz as a wine solid. 1H NMR ($CDCl_3$, 300 MHz) δ (ppm): 8.03 (s, 2H), 7.57 (d, $J = 3.9$ Hz, 2H), 7.35 (s, 2H), 7.13 (d, $J = 3.9$ Hz, 2H), 3.08 (m, 4H), 1.90–1.87 (m, 4H), 1.54–1.31 (m, 20H), 0.89 (m, 6H). MS (APCI): calcd 838.8, found $(M + 1)^+$ 839.4. Anal. Calcd for $C_{40}H_{42}Br_2N_2S_4$ (%): C 57.27, H 5.05, N 3.34, S 15.29. Found (%): C 57.23, H 5.45, N 3.23, S 14.38.

Synthesis of PFTTQx. 2,7-Bis(4,4,5,5-tetramethyl-1,3,2-dioxaborolan-2-yl)-9,9-dioctylfluorene (**8**) (0.321 g, 0.5 mmol), TTQx (0.420 g 0.5 mmol), tris(dibenzylideneacetone)dipalladium(0) ($Pd_2(dba)_3$) (4.5 mg), and tri(*o*-tolyl)phosphine (9.0 mg) ($P(o-Tol)_3$) were dissolved in a mixture of toluene (10 mL), THF (5 mL), and 20% aqueous tetraethylammonium hydroxide (4 mL) in a 50 mL two-necked round-bottomed flask under argon. The mixture was refluxed with vigorous stirring in the dark for 20 h under an argon atmosphere. After cooling to room temperature, the mixture was poured into methanol. The precipitated material was collected by filtration through a funnel. After washing with acetone for 24 h in a Soxhlet apparatus to remove oligomers and catalyst residues, the resulting material was dissolved in 30 mL of 1,2-dichlorobenzene (ODCB). The solution was filtered with a 0.45 μm PTFE filter, concentrated, and precipitated from methanol to yield PFTTQx as a wine solid (680 mg, 85%). 1H NMR ($CDCl_3$, 300 Hz) δ (ppm): 8.08–8.04 (m, 2H), 7.94–7.88 (m, 2H), 7.78–7.75 (m, 6H), 7.61–7.45 (m, 4H), 6.79–6.72 (m, 2H), 2.97–2.88 (m, 4H), 2.11–2.05 (m, 4H), 1.87–1.80 (m, 4H), 1.50–1.13 (m, 44H), 0.89–0.75 (m, 12H). GPC (1,2,4-trichlorobenzene, polystyrene standard): $M_n = 10.8$ kg mol^{-1} , $M_w = 22.6$ kg mol^{-1} , PDI = 2.09. Anal. Calcd for $(C_{69}H_{84}N_2S_4)_n$ (%): C 77.47, H 7.91, N 2.61, S 11.99. Found (%): C 78.51, H 8.55, N 2.50, S 10.91.

Synthesis of PFTTPz. PFTTPz was prepared according to the same procedure as that for PFTTQx. 51% yield. 1H NMR (ODCB-*d*₄, 300 Hz) δ (ppm): 8.03–7.63 (m, 6H), 7.50–7.20 (m, 2H), 7.20–7.10 (m, 2H), 6.89–6.78 (m, 2H), 6.79–6.72 (m, 2H), 3.01–2.90 (m, 4H), 2.25–1.91 (m, 4H), 1.90–1.70 (m, 4H), 1.50–1.10 (m, 44H), 0.89–0.75 (m, 12H). GPC (1,2,4-trichlorobenzene, polystyrene standard): $M_n = 11.7$ kg mol^{-1} , $M_w = 31.1$ kg mol^{-1} , PDI = 2.66. Anal. Calcd for $(C_{69}H_{82}N_2S_4)_n$ (%): C 77.63, H 7.93, N 2.62, S 12.01. Found (%): C 76.14, H 8.50, N 2.36, S 10.58.

Synthesis of PCzTTQx. PCzTTQx was prepared according to the same procedure as that for PFTTQx. 89% yield. 1H NMR ($CDCl_3$, 300 Hz) δ (ppm): 8.09–7.90 (m, 6H), 7.75–7.68 (m, 4H), 7.53–7.39 (m, 4H), 6.77–6.73 (m, 2H), 4.71 (br, 1H), 2.94

(br, 4H), 2.94 (br, 2H), 2.25–2.22 (m, 2H), 1.85–1.81 (m, 4H), 1.47–1.15 (m, 44H), 0.90–0.85 (m, 6H), 0.80–0.76 (m, 6H). GPC (1,2,4-trichlorobenzene, polystyrene standard): $M_n = 10.7 \text{ kg mol}^{-1}$, $M_w = 25.8 \text{ kg mol}^{-1}$, PDI = 2.41. Anal. Calcd for $(\text{C}_{69}\text{H}_{85}\text{N}_3\text{S}_4)_n$ (%): C 76.40, H 7.90, N 3.87, S 11.82. Found (%): C 76.10, H 8.40, N 3.67, S 11.43.

Synthesis of PCzTTPz. PCzTTPz was prepared according to the same procedure as that for PFTTQx. 51% yield. ^1H NMR (ODCB- d_4 , 400 Hz) δ (ppm): 8.09–7.90 (m, 4H), 7.75–7.68 (m, 4H), 7.53–7.39 (m, 4H), 6.77–6.73 (m, 2H), 4.71 (br, 1H), 3.64 (br, 4H), 2.94 (br, 2H), 2.25–2.22 (m, 2H), 1.85–1.81 (m, 4H), 1.47–1.15 (m, 44H), 0.90–0.55 (m, 12H). GPC (1,2,4-trichlorobenzene, polystyrene standard): $M_n = 16.6 \text{ kg mol}^{-1}$, $M_w = 46.0 \text{ kg mol}^{-1}$, PDI = 2.77. Anal. Calcd for $(\text{C}_{69}\text{H}_{83}\text{N}_3\text{S}_4)_n$ (%): C 76.55, H 7.73, N 3.88, S 11.85. Found (%): C 76.02, H 8.21, N 3.71, S 11.58.

Measurement and Characterization. ^1H and ^{13}C NMR were recorded using a Bruker-300 or 400 spectrometer operating at 300 or 400 and 75 MHz in deuterated chloroform solution or ODCB at 298 K. Chemical shifts were reported as δ values (ppm) relative to an internal tetramethylsilane (TMS) standard. Mass (MS) experiments were performed on an Esquire HCT PLUS. The number-average molecular weights (M_n) and weight-average molecular weights (M_w) were determined at 150 °C by a PL-GPC 220 type in 1,2,4-trichlorobenzene using a calibration curve with standard polystyrene as a reference. Elemental analyses were performed on a Vario EL elemental analysis instrument (Elementar Co.). Differential scan calorimetry (DSC) measurements were carried out with a Netzsch DSC 204 under N_2 flow at heating and cooling rates of 10 °C min^{-1} . Thermogravimetric analyses (TGA) were carried out with a Netzsch TG 209 under N_2 flow at a heating rate of 10 °C min^{-1} . UV–vis absorption spectra were performed on a HP 8453 spectrophotometer. Cyclic voltammetry (CV) was performed on a CHI600D electrochemical workstation with a platinum working electrode and a Pt wire counter electrode at a scan rate of 50 mV s^{-1} against an Ag/AgCl (3 M of KCl in acetonitrile) reference electrode with a nitrogen-saturated anhydrous solution of 0.1 mol L^{-1} tetrabutylammonium hexafluorophosphate (Bu_4NPF_6) in acetonitrile. Atom force microscopy (AFM) measurements were carried out using a Digital Instrumental DI Multimode Nanoscope IIIa in tapping mode.

Solar Cell Device Fabrication and Characterization. The organic photovoltaic cells was constructed in the form of the sandwiched structure of glass/indium tin oxide (ITO)/poly(3,4-ethylenedioxythiophene polystyrenesulfonate (PEDOT:PSS)/copolymer:PC₇₁BM/Ba/Al. Prior to use, the ITO-coated glass substrates were cleaned by ultrasonic treatment in deionized water, acetone, and isopropyl alcohol and dried in a nitrogen stream, followed by an oxygen plasma treatment. To fabricate photovoltaic devices, a thin layer (ca. 40 nm) of PEDOT:PSS (Baytron P VP Al 4083, filtered at 0.45 μm) was spin-coated on the precleaned glass substrates at 5000 rpm and baked at 140 °C for 10 min under ambient conditions. The substrates were then transferred into an argon-filled glovebox. Subsequently, the copolymer:PC₇₁BM active layer (ca. 80 nm for PFTTQx and PCzTTQx and 95 nm for PFTTPz and PCzTTPz) was spin-coated on the PEDOT:PSS layer at 1000 rpm from a homogeneously blend solution. The solution was prepared by dissolving the copolymers (2 mg mL^{-1}) and PC₇₁BM (8 mg mL^{-1}) in a ODCB solvent mixture for PFTTQx and PFTTPz and the copolymers (2 mg mL^{-1}) and PC₇₁BM (4 mg mL^{-1}) in a ODCB solvent mixture for PCzTTQx and PCzTTPz and filtered with a 0.2 μm PTFE filter. The substrates were annealed at 150 °C for 10 min prior to electrode deposition. To complete device fabrication, the substrates were pumped down to a high vacuum (1×10^{-6} Torr), and barium (9 nm) topped with aluminum (100 nm) was thermally evaporated onto the active layer through shadow masks. The effective devices area was measured to be 0.15 cm^2 .

The current density–voltage (J – V) characteristics were recorded with a Keithley 236 source meter. The spectral response was measured with a commercial photomodulation spectroscopic setup (Oriol). A calibrated Si photodiode was used to determine the photosensitivity. The EQE of the devices was measured on a Hypermonolight System (Bunkoh-Keiki SM-250).

Results and Discussion

Synthesis and Characterization. The synthetic routes of the monomers and copolymers are shown in Schemes 1 and 2, respectively. Monomers 2,7-bis(4,4,5,5-tetramethyl-1,3,2-dioxaborolan-2-yl)-9,9-dioctylfluorene (**8**) and 2,7-bis(4',4',5',5'-tetramethyl-1',3',2'-dioxaborolan-2'-yl)-*N*-9'-heptadecanilycarbazole (**9**) were prepared according to the published literature.^{20,22} Condensation of 1,2-bis(5-octylthiophen-2-yl)ethane-1,2-dione (**1**)⁴² and 3,6-dibromobenzene-1,2-diamine (**2**)¹⁸ in acetic acid yielded 5,8-dibromo-2,3-bis(5-octylthiophen-2-yl)-quinoxaline (**3**) in high yield of 91%. 2,3-Bis(5-octylthiophen-2-yl)-5,8-di(thiophen-2-yl)quinoxaline (**5**) was synthesized by Stille coupling of 1 equiv of compound **3** and 2 equiv of 2-(tributylstannyl)thiophene (**4**) with 92% yield. 8,11-Dibromo-2,5-dioctyldithieno[2,3-*a*:3',2'-*c*]phenazine (**6**) was synthesized from compound **3** by oxidative cyclization using FeCl_3 in $\text{CH}_2\text{Cl}_2/\text{CH}_3\text{NO}_2$ as oxidizing agent with a yield of 28%. 2,5-Dioctyl-8,11-di(thiophen-2-yl)dithieno[2,3-*a*:3',2'-*c*]phenazine (**7**) was synthesized from compound **6** by Stille coupling with compound **4**. Different from the synthesis of compound **5**, $\text{Pd}(\text{PPh}_3)_4$ was used as the catalyst instead of $\text{Pd}(\text{PPh}_3)_2\text{Cl}_2$ because it was found that compound **7** can be obtained in a much higher yield by using $\text{Pd}(\text{PPh}_3)_4$ as catalyst than that of using $\text{Pd}(\text{PPh}_3)_2\text{Cl}_2$ catalyst. The key monomers 5,8-bis(5-bromothiophen-2-yl)-2,3-bis(5-octylthiophen-2-yl)quinoxaline (TTQx) and 8,11-bis(5-bromothiophen-2-yl)-2,5-dioctyldithieno[2,3-*a*:3',2'-*c*]phenazine (TTPz) were obtained by bromination of compound **5** or **7** with NBS in THF, respectively.

D–A type copolymers PFTTQx, PFTTPz, PCzTTQx, and PCzTTPz were synthesized by Suzuki polycondensation of TTQx or TTPz with monomer **8** or **9**, respectively. It was found that high molecular weight copolymers can be obtained by using tris(dibenzylideneacetone)dipalladium(0) ($\text{Pd}_2(\text{dba})_3$)/tri(*o*-tolyl)phosphine ($\text{P}(\text{o-Tol})_3$) as the catalyst system,⁴³ whereas the reaction based on commonly used $\text{Pd}(\text{PPh}_3)_4$ catalyst can only offer low molecular weight copolymers. PFTTQx and PCzTTQx have excellent solubility in common organic solvents such as THF, chloroform, and chlorobenzene, etc., due to their pendant substituted thiophene groups which can decrease the intermolecular packing of the copolymers and enhance the copolymers' solubility, while the solubility of copolymers based on polycyclic aromatic ring PFTTPz and PCzTTPz are low in common organic solvents and are only soluble in solvents such as ODCB and 1,2,4-trichlorobenzene. The M_n of the copolymers were determined by gel permeation chromatography (GPC) in 1,2,4-trichlorobenzene using polystyrene as standard. The M_n of PFTTQx, PFTTPz, PCzTTQx, and PCzTTPz are 10.8, 11.7, 10.7, and 16.6 kg mol^{-1} , with the corresponding polydispersity index (PDI) of 2.09, 2.66, 2.41, and 2.71, respectively. The thermal properties of the copolymers were investigated by using DSC and TGA. As shown in Table 1, all the copolymers have good thermal stability with 5% weight-loss temperature (T_d) of 431, 439, 433, and 442 °C for PFTTQx, PFTTPz, PCzTTQx, and PCzTTPz, respectively. The glass transition temperature (T_g) are 92.6 and 100.5 °C for PFTTPz and PCzTTPz, respectively, which are higher than

those of PFTTQx and PCzTTQx, probably due to their more rigid main chain caused by the incorporated planarized polycyclic aromatics.^{40,41}

Optical Properties. The photophysical properties of the copolymers were investigated both in ODCB solution and in thin films, which are shown in Figure 1 and Table 2. All of the copolymers showed two absorption peaks, which is a common feature of D–A copolymers. The absorption peaks at short wavelength (399–427 nm) originate from π – π^* transition of their conjugated backbone, while the absorption peaks at long wavelength (537–609 nm) could be attributed to the strong intramolecular charge transfer (ICT) interaction between the fluorene/carbazole donors and the TTQx/TPPz acceptors.³⁴ It was found that the copolymers based on thiophene-substituted quinoxaline exhibit an obviously red-shifted ICT absorbance peak compared to those D–A copolymers based on phenyl-substituted quinoxaline. For example, PFTTQx has a maximum absorption peak at around 561 nm, while it was reported that another analogous copolymer based on phenyl-substituted quinoxaline APFO-15 possessed the absorption peak at 542 nm.^{18,32} Similarly, PCzTTQx also exhibits a much red-shifted absorption peak (more than 30 nm) compared to its analogous copolymer poly{*N*-[1-(2'-ethylhexyl)-3-ethylheptanyl]carbazole-2,7-diyl-*alt*-5,8-dithien-2-yl-2,3-diphenylquinoxaline-5',5''-diyl} (PC-DTQx).³⁴ All of these results indicate that the band gap of quinoxaline-based D–A copolymers can be effectively lowered by changing the pendant substituted groups from benzene into thiophene. Interestingly, compared to PFTTQx and PCzTTQx, copolymers PFTTPz and PCzTTPz exhibit more pronounced red-shifted absorption spectrum with peaks at around 635 nm, which is due to the enlarged

planar polycyclic aromatic ring of TPPz acceptor. The absorption spectra in the solid state of copolymers are red-shifted 20–35 nm compared with their corresponding spectra in solution, indicating the presence of strong intermolecular interactions in the solid state. As shown in Table 2, the optical bandgaps (E_g^{opt}) of the copolymers calculated from the absorption onset in the films are 1.86 eV for PFTTQx, 1.68 eV for PFTTPz, 1.90 eV for PCzTTQx, and 1.66 eV for PCzTTPz. Clearly, the photophysical properties and band gap of those copolymers can be easily tuned by using TTQx or TPPz as the acceptors.

Electrochemical Properties. The electrochemical behaviors of the copolymers were investigated by cyclic voltammetry (CV). The CV was performed in a solution of tetrabutylammonium hexafluorophosphate (Bu_4NPF_6) (0.1 M) in acetonitrile, using Ag/AgCl and a platinum wire as reference and counter electrode, respectively, at a scan rate of 50 mV/s at room temperature. A platinum electrode coated with thin copolymer film was used as the working electrode. The potential of ferrocene/ferrocenium (Fc/Fc^+) was measured to be -0.06 V to the Ag/Ag⁺ electrode under the same conditions. It is assumed that the redox potential of Fc/Fc^+ has an absolute energy level of -4.8 eV to vacuum.^{44,45} Thus, the HOMO of the copolymers was calculated according to the following equation

$$E_{\text{HOMO}} = -e(E_{\text{ox}} + 4.86) \text{ (eV)}$$

where E_{ox} is the onset oxidation potential vs Ag/Ag⁺. The HOMO energy values of PFTTQx and PCzTTQx were calculated to be -5.26 and -5.23 eV, respectively, which are around 0.1 eV higher than those of their analogous copolymers APFO-15 and PC-DTQx.^{32,34} This is probably due to the thiophene rings among them, which has a stronger electron-donating ability compared to the benzene rings among APFO-15 and PC-DTQx. The copolymers PFTTPz and PCzTTPz show a slightly increased HOMO energy values of -5.21 and -5.17 eV, respectively, compared to PFTTQx and PCzTTQx. It has been reported that V_{oc} of PSCs relates with the difference between the HOMO level of electron donor and the lowest unoccupied molecular orbital

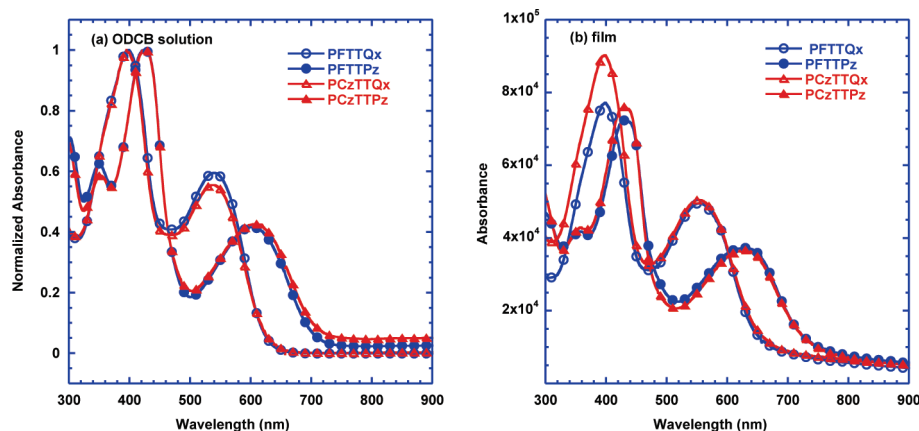


Figure 1. Absorption spectra of PFTTQx, PFTTPz, PCzTTQx, and PCzTTPz (a) in ODCB solution and (b) in film.

Table 2. Electrochemical and Optical Properties of the Polymers

| copolymers | λ_{abs} (nm) solution | λ_{abs} (nm) film | E_g^{opt} (eV) | E_{ox} (V) | E_{HOMO} (eV) | E_{LUMO} (eV) | μ ($\text{cm}^2 \text{V}^{-1} \text{s}^{-1}$) |
|------------|--------------------------------------|----------------------------------|-------------------------|---------------------|------------------------|------------------------|---|
| PFTTQx | 399, 540 | 401, 561 | 1.86 | 0.40 | -5.26 | -3.40 | 1.04×10^{-4} |
| PFTTPz | 424, 600 | 440, 635 | 1.68 | 0.35 | -5.21 | -3.53 | 5.68×10^{-4} |
| PCzTTQx | 395, 537 | 400, 556 | 1.90 | 0.37 | -5.23 | -3.33 | 5.68×10^{-5} |
| PCzTTPz | 427, 609 | 438, 635 | 1.66 | 0.31 | -5.17 | -3.51 | 5.43×10^{-4} |

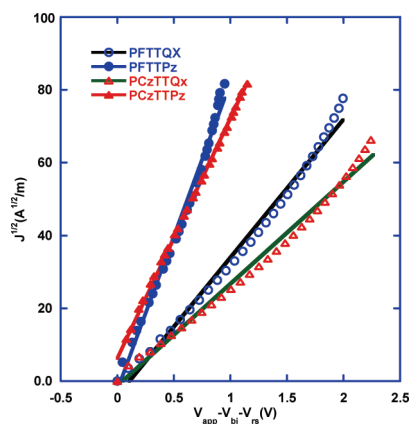


Figure 2. $J^{1/2}$ vs V characteristics of devices in Au/MoO₃/copolymer/PEDOT:PSS/ITO configuration. The solid lines represent the fitting curves.

(LUMO) level of electron acceptor.⁴⁶ Thus, the relative low HOMO levels of these copolymers may ensure them a high V_{oc} when used as donors in PSCs. The LUMO energy levels of the copolymers were estimated from the HOMO energy levels and E_g^{opt} using the equation

$$E_{LUMO} = E_{HOMO} + E_g^{opt}$$

As shown in Table 2, PFTTPz and PCzTTPz exhibit obviously decreased LUMO levels compared to PFTTQx and PCzTTQx. The LUMO levels of PFTTPz and PCzTTPz are -3.53 and -3.51 eV, respectively, whereas PFTTQx and PCzTTQx' LUMO levels are around -3.3 to -3.4 eV. The relative large offsets between the LUMO levels of all the copolymers and PC₇₁BM (-3.91 eV)⁴⁷ indicate that charge transfer from the copolymers to PC₇₁BM would be efficient.

Hole Mobility. The hole mobility of the donor conjugated polymers plays a key role in the performance of BHJ-type PSCs. In order to get some ideas about the influence of the materials' chemical structures on their charge transporting properties, the hole mobility of the copolymers is measured by using the space charge limited current (SCLC) method, which has been extensively used to investigate the charge transport properties of the PSCs active layer.^{48,49} Figure 2 shows the $J^{1/2}$ – V characteristics of the copolymers obtained in the dark for hole-only devices with the configuration: Au/MoO₃/copolymer/PEDOT:PSS/ITO. The perfect linear fitting in the figure indicates the $J^{1/2}$ – V characteristic follows the Mott–Gurney square law in the region from ~ 0 to 2.5 V

$$J = \frac{9}{8} \epsilon_0 \epsilon_r \mu_0 \frac{V^2}{L^3}$$

where J is the current, μ is the hole mobility, ϵ_0 is the permittivity of free space, ϵ_r is the dielectric constant of the polymer, L is the thickness of the active layer, and V is the voltage drop across the device. $V = V_{appl} - V_{rs} - V_{bi}$, where V is the effective voltage, V_{appl} is the applied voltage, V_{rs} is the voltage drop, and V_{bi} is the built-in voltage.

Table 2 shows the hole mobilities of the copolymers obtained by the SCLC method. It was found that the mobilities of the copolymers can be dramatically enhanced by adjusting the pendant substituted groups on the quinoxaline acceptor. PFTTQx, the copolymers based on thiophene-substituted quinoxaline acceptors, has a hole mobility of $1.04 \times 10^{-4} \text{ cm}^2 \text{ V}^{-1} \text{ s}^{-1}$, while its analogous copolymer PFTTPz with planar cyclic aromatic ring acceptors shows a much improved hole mobility of $5.68 \times 10^{-4} \text{ cm}^2 \text{ V}^{-1} \text{ s}^{-1}$.

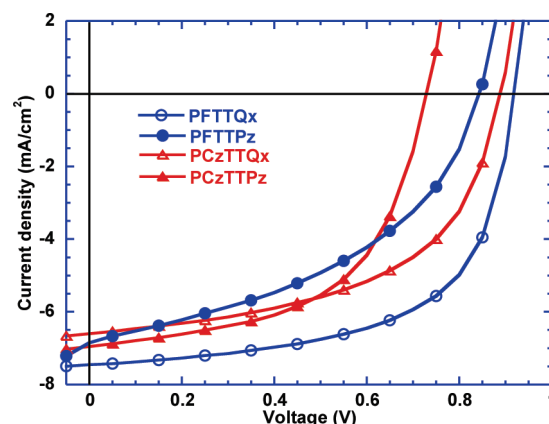


Figure 3. J – V characteristics of the devices with the structure of ITO/PEDOT:PSS/copolymer:PC₇₁BM/Ba/Al under the illumination of AM 1.5G from a solar simulator (900 W m^{-2}).

Table 3. Photovoltaic Performance of the Polymers Measured under the Illumination of Simulated AM 1.5G Conditions (900 W m^{-2})

| copolymers | J_{sc} (mA cm^{-2}) | V_{oc} (V) | FF | PCE (%) |
|---------------------------|----------------------------------|--------------|------|---------|
| PFTTQx (1:4) ^a | 7.4 | 0.90 | 0.59 | 4.4 |
| PFTTPz (1:4) | 4.7 | 0.85 | 0.51 | 2.1 |
| PCzTTQx (1:2) | 6.6 | 0.88 | 0.53 | 3.5 |
| PCzTTPz (1:2) | 6.4 | 0.75 | 0.54 | 3.0 |

^a Blend ratio of polymer:PC₇₁BM.

Similar improvement on the mobilities was also observed among the carbazole-based copolymers. The hole mobility of PCzTTPz ($5.43 \times 10^{-4} \text{ cm}^2 \text{ V}^{-1} \text{ s}^{-1}$) is almost 1 order of magnitude greater than that of PCzTTQx ($5.68 \times 10^{-5} \text{ cm}^2 \text{ V}^{-1} \text{ s}^{-1}$). Clearly, the pendant substituted thiophene groups on the quinoxaline rings among PFTTQx and PCzTTQx can potentially hindered the intermolecular packing of the copolymers and reduces their carrier mobility. After oxidize cyclization, the two pendant substituted thiophene rings are connected together, which results in an enlarged fused planar aromatic ring. Thereby, the π – π interaction among the resulting copolymers PFTTPz and PCzTTPz are enhanced and the mobilities are improved, which is favorable for PSCs application.^{41,50}

Photovoltaic Properties. Photovoltaic properties of the copolymers were investigated in solar cells with device structure of ITO/PEDOT:PSS/copolymer:PC₇₁BM/Ba/Al. The copolymer:PC₇₁BM blend films are prepared from ODCB solution. Figure 3 shows the J – V characteristics of the polymer solar cells under AM 1.5G condition at 900 W m^{-2} . Representative characteristics of the solar cells are summarized in Table 3. All of the copolymers show excellent photovoltaic properties with overall efficiencies over 2%. It was found that both PFTTPz and PCzTTPz exhibited a slightly decreased V_{oc} compared to those of PFTTQx and PCzTTQx, which is consistent with their relative high HOMO levels (Table 2). Among all the copolymers, PFTTQx showed the best performance with a PCE of 4.4%, a V_{oc} of 0.90 V, a J_{sc} of 7.4 mA cm^{-2} , and a FF of 0.59, while its analogous copolymer PFTTPz only exhibited a PCE of 2.1% with a V_{oc} of 0.85 V, a J_{sc} of 4.7 mA cm^{-2} , and a FF of 0.51. Both the carbazole-based copolymers PCzTTQx and PCzTTPz show good PSCs device performances with PCEs more than 3.0%. To confirm the PCE, the external quantum efficiency (EQE) of the device based on PFTTQx:PC₇₁BM illuminated by monochromatic light was determined and shown in Figure 4. The device based on the PFTTQx:PC₇₁BM blend shows very

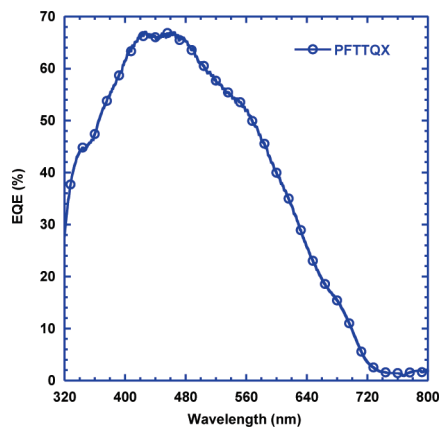


Figure 4. EQE spectrum of PFTTQx-based solar cell illuminated by monochromatic light.

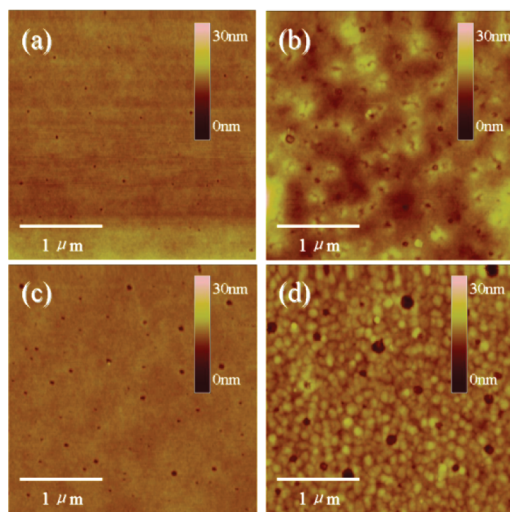


Figure 5. AFM images: (a), (b), (c), and (d) are height images for PFTTQx, PFTTPz, PCzTTQx, and PCzTTPz, respectively. All the images are $3\ \mu\text{m} \times 3\ \mu\text{m}$.

efficient photoresponse in the broad range from 320 to 700 nm. The high EQE over 40% was observed in a very broad range from 330 to 600 nm. The integral of the EQE is in accordance with J_{sc} measured from the devices.

It should be noted that both PFTTPz and PCzTTPz exhibited lower PCEs compared to PFTTQx and PCzTTQx, respectively, despite their much higher hole mobilities and more red-shifted absorbance. We speculate that it is probably due to their poor solubility caused by the rigid fused planar aromatic rings which will affect the morphology of copolymer:PC₇₁BM blend films and further influence the charge separation efficiency of the devices.^{51,52} AFM was used to characterize the film morphology of copolymer:PC₇₁BM blends. The resulted topography images are shown in Figure 5. As shown in Figures 5a and 5c, the surface of PFTTQx:PC₇₁BM and PCzTTQx:PC₇₁BM blend films are quite smooth, with root-mean-square roughness (rms) of 0.445 and 0.518 nm, respectively. This indicates good miscibility between PFTTQx, PCzTTQx, and PC₇₁BM without large phase separation, and the resulting blend films may exhibit good film morphology with a smaller domain size approaching the ideal domain size of 5–10 nm,⁶ resulting in the increase of J_{sc} and FF. However, the surfaces of PFTTPz:PC₇₁BM and PCzTTPz:PC₇₁BM blend films are very rough, with rms of 1.807 and 1.604 nm, respectively. The large

domains (larger than 100 nm) on the surface of the film indicate a nonoptimal morphology, which is not favorable for charge separation from the copolymers to PC₇₁BM and thus limits the efficiencies of the resulted devices.⁵³ The more rigid main chains of PFTTPz and PCzTTPz compared to PFTTQx and PCzTTQx could lead to higher crystallinity in thin film, thus promoting their hole mobilities. However the high crystallinity of PFTTPz and PCzTTPz also greatly increased the phase separation in blended thin films with PC₇₁BM, as can be observed in the respective AFM images (Figures 5b and 5d). The gain from higher mobility cannot compensate for the loss due to nonideal phase separation; thus, the overall device performances of PFTTPz and PCzTTPz were worse than those of PFTTQx and PCzTTQx. Similar problems with highly rigid donor materials are also reported by Bao et al.⁵⁴

Conclusion

In conclusion, a series of D–A copolymers PFTTQx, PFTTPz, PCzTTQx, and PCzTTPz have been successfully developed. The copolymers based on thiophene-substituted quinoxaline acceptors PFTTQx and PCzTTQx show red-shifted absorption spectra compared to previously reported benzene-substituted quinoxaline copolymers. Moreover, the D–A copolymers of PFTTPz and PCzTTPz based on the polycyclic aromatic ring exhibit significant red shift absorption with a smaller band gap of 1.68 and 1.66 eV, respectively. The mobilities of PFTTPz and PCzTTPz are much higher than their analogous copolymers PFTTQx and PCzTTQx due to the enlarged fused planar aromatic ring among them. BHJ PSCs based on the blend of the copolymers with PC₇₁BM show promising performance with overall efficiencies more than 2%. Despite their much higher mobility and more red-shifted absorbance, it was found that both PFTTPz and PCzTTPz exhibited lower PCEs compared to PFTTQx and PCzTTQx due to their poor solubility which results in nonideal phase separation. Among all the copolymers, PFTTQx shows the best performance with a PCE of 4.4%, a V_{oc} of 0.90 V, a J_{sc} of $7.4\ \text{mA cm}^{-2}$, and a FF of 0.59.

Acknowledgment. The work was financially supported by the Natural Science Foundation of China (No. 50990065, 51010003, 51073058, and 20904011), the Ministry of Science and Technology, China (MOST) National Research Project (No. 2009CB623601), and the Fundamental Research Funds for the Central Universities, South China University of Technology (No. 2009220012).

Supporting Information Available: Thermal properties and electrochemical properties of the copolymers. This material is available free of charge via the Internet at <http://pubs.acs.org>.

References and Notes

- (1) Yu, G.; Gao, J.; Hummelen, J. C.; Wudl, F.; Heeger, A. J. *Science* **1995**, *270*, 1789–1791.
- (2) Cheng, Y.-J.; Yang, S.-H.; Hsu, C.-S. *Chem. Rev.* **2009**, *109*, 5868–5923.
- (3) Coakley, K. M.; McGehee, M. D. *Chem. Mater.* **2004**, *16*, 4533–4542.
- (4) Brabec, C. J.; Sariciftci, N. S.; Hummelen, J. C. *Adv. Funct. Mater.* **2001**, *11*, 15–26.
- (5) Gunes, S.; Neugebauer, H.; Sariciftci, N. S. *Chem. Rev.* **2007**, *107*, 1324–1338.
- (6) Thompson, B. C.; Frechet, J. M. J. *Angew. Chem., Int. Ed.* **2008**, *47*, 58–77.
- (7) Chen, J.; Cao, Y. *Acc. Chem. Res.* **2009**, *42*, 1709–1718.
- (8) Wienk, M. M.; Kroon, J. M.; Verhees, W. J. H.; Knol, J.; Hummelen, J. C.; van Hal, P. A.; Janssen, R. A. J. *Angew. Chem., Int. Ed.* **2003**, *42*, 3371–3375.

- (9) Ma, W. L.; Yang, C. Y.; Gong, X.; Lee, K.; Heeger, A. J. *Adv. Funct. Mater.* **2005**, *15*, 1617–1622.
- (10) Li, G.; Shrotriya, V.; Huang, J. S.; Yao, Y.; Moriarty, T.; Emery, K.; Yang, Y. *Nature Mater.* **2005**, *4*, 864–868.
- (11) Wang, W. L.; Wu, H. B.; Yang, C. Y.; Luo, C.; Zhang, Y.; Chen, J. W.; Cao, Y. *Appl. Phys. Lett.* **2007**, *90*, 183512.
- (12) Huo, L.; Hou, J.; Zhang, S.; Chen, H.-Y.; Yang, Y. *Angew. Chem., Int. Ed.* **2010**, *122*, 1542–1545.
- (13) He, Y.; Chen, H.-Y.; Hou, J.; Li, Y. *J. Am. Chem. Soc.* **2010**, *132*, 1377–1382.
- (14) Zhao, G.; He, Y.; Li, Y. *Adv. Mater.* **2010**, *22*, 4355–4358.
- (15) Li, Y. F.; Zou, Y. P. *Adv. Mater.* **2008**, *20*, 2952–2958.
- (16) Svensson, M.; Zhang, F. L.; Veenstra, S. C.; Verhees, W. J. H.; Hummelen, J. C.; Kroon, J. M.; Inganäs, O.; Andersson, M. R. *Adv. Mater.* **2003**, *15*, 988–991.
- (17) Zhou, Q. M.; Hou, Q.; Zheng, L. P.; Deng, X. Y.; Yu, G.; Cao, Y. *Appl. Phys. Lett.* **2004**, *84*, 1653–1655.
- (18) Gadisa, A.; Mammo, W.; Andersson, L.; Admassie, S.; Zhang, F.; Andersson, M.; Inganäs, O. *Adv. Funct. Mater.* **2007**, *17*, 3836–3842.
- (19) Zhang, F.; Bijleveld, J.; Perzon, E.; Tvingstedt, K.; Barrau, S.; Inganäs, O.; Andersson, M. R. *J. Mater. Chem.* **2008**, *18*, 5468–5474.
- (20) Wang, E. G.; Wang, M.; Wang, L.; Duan, C. H.; Zhang, J.; Cai, W. Z.; He, C.; Wu, H. B.; Cao, Y. *Macromolecules* **2009**, *42*, 4410–4415.
- (21) Huang, F.; Chen, K.-S.; Yip, H.-L.; Hau, S. K.; Acton, O.; Zhang, Y.; Luo, J.; Jen, A. K. Y. *J. Am. Chem. Soc.* **2009**, *131*, 13886–13887.
- (22) Blouin, N.; Michaud, A.; Leclerc, M. *Adv. Mater.* **2007**, *19*, 2295–2300.
- (23) Park, S. H.; Roy, A.; Beaupre, S.; Cho, S.; Coates, N.; Moon, J. S.; Moses, D.; Leclerc, M.; Lee, K.; Heeger, A. J. *Nature Photonics* **2009**, *3*, 297–303.
- (24) Wang, E. G.; Wang, L.; Lan, L. F.; Luo, C.; Zhuang, W. L.; Peng, J. B.; Cao, Y. *Appl. Phys. Lett.* **2008**, *92*, 033307.
- (25) Duan, C. H.; Cai, W. Z.; Huang, F.; Zhang, J.; Wang, M.; Yang, T. B.; Zhong, C. M.; Gong, X.; Cao, Y. *Macromolecules* **2010**, *43*, 5262–5268.
- (26) Qin, R.; Li, W.; Li, C.; Du, C.; Veit, C.; Schleiermacher, H.-F.; Andersson, M.; Bo, Z.; Liu, Z.; Inganäs, O.; Wuerfel, U.; Zhang, F. *J. Am. Chem. Soc.* **2009**, *131*, 14612–14613.
- (27) Peet, J.; Kim, J. Y.; Coates, N. E.; Ma, W. L.; Moses, D.; Heeger, A. J.; Bazan, G. C. *Nature Mater.* **2007**, *6*, 497–500.
- (28) Hou, J.; Chen, H.-Y.; Zhang, S.; Li, G.; Yang, Y. *J. Am. Chem. Soc.* **2008**, *130*, 16144–16145.
- (29) Liang, Y. Y.; Xu, Z.; Xia, J. B.; Tsai, S. T.; Wu, Y.; Li, G.; Ray, C.; Yu, L. P. *Adv. Mater.* **2010**, *22*, E135–E138.
- (30) Zou, Y. P.; Najari, A.; Berrouard, P.; Beaupre, S.; Aich, B. R.; Tao, Y.; Leclerc, M. *J. Am. Chem. Soc.* **2010**, *132*, 5330–5331.
- (31) Piliago, C.; Holcombe, T. W.; Douglas, J. D.; Woo, C. H.; Beaujuge, P. M.; Frechet, J. M. J. *J. Am. Chem. Soc.* **2010**, *132*, 7595–7597.
- (32) Kitazawa, D.; Watanabe, N.; Yamamoto, S.; Tsukamoto, J. *Appl. Phys. Lett.* **2009**, *95*, 053701.
- (33) Lindgren, L. J.; Zhang, F.; Andersson, M.; Barrau, S.; Hellstrom, S.; Mammo, W.; Perzon, E.; Inganäs, O.; Andersson, M. R. *Chem. Mater.* **2009**, *21*, 3491–3502.
- (34) Zhou, E.; Cong, J.; Tajima, K.; Hashimoto, K. *Chem. Mater.* **2010**, *22*, 4890–4895.
- (35) Wang, E.; Hou, L.; Wang, Z.; Hellström, S.; Zhang, F.; Inganäs, O.; Andersson, M. R. *Adv. Mater.* **2010**, *22*, 5240–5244.
- (36) Huo, L.; Tan, Z.; Wang, X.; Zhou, Y.; Han, M.; Li, Y. *J. Polym. Sci., Part A: Polym. Chem.* **2008**, *46*, 4038–4049.
- (37) Yamamoto, T.; Zhou, Z. H.; Kanbara, T.; Shimura, M.; Kizu, K.; Maruyama, T.; Nakamura, Y.; Fukuda, T.; Lee, B. L.; Ooba, N.; Tomaru, S.; Kurihara, T.; Kaino, T.; Kubota, K.; Sasaki, S. *J. Am. Chem. Soc.* **1996**, *118*, 10389–10399.
- (38) Peng, Q.; Xu, J.; Zheng, W. *J. Polym. Sci., Part A: Polym. Chem.* **2009**, *47*, 3399–3408.
- (39) Xiao, S.; Stuart, A. C.; Liu, S.; You, W. *ACS Appl. Mater. Interfaces* **2009**, *1*, 1613–1621.
- (40) Xiao, S.; Stuart, A. C.; Liu, S.; Zhou, H.; You, W. *Adv. Funct. Mater.* **2010**, *20*, 635–643.
- (41) Mondal, R.; Becerril, H. A.; Verploegen, E.; Kim, D.; Norton, J. E.; Ko, S.; Miyaki, N.; Lee, S.; Toney, M. F.; Bredas, J.-L.; McGehee, M. D.; Bao, Z. *J. Mater. Chem.* **2010**, *20*, 5823–5834.
- (42) Babudri, F.; Fiandanese, V.; Marchese, G.; Punzi, A. *Tetrahedron Lett.* **1995**, *36*, 7305–7308.
- (43) Murage, J.; Eddy, J. W.; Zimbalist, J. R.; McIntyre, T. B.; Wagner, Z. R.; Goodson, F. E. *Macromolecules* **2008**, *41*, 7330–7338.
- (44) Li, Y. F.; Cao, Y.; Gao, J.; Wang, D. L.; Yu, G.; Heeger, A. J. *Synth. Met.* **1999**, *99*, 243–248.
- (45) Pommerehne, J.; Vestweber, H.; Guss, W.; Mahrt, R. F.; Bassler, H.; Porsch, M.; Daub, J. *Adv. Mater.* **1995**, *7*, 551–554.
- (46) Scharber, M. C.; Wühlbacher, D.; Koppe, M.; Denk, P.; Waldauf, C.; Heeger, A. J.; Brabec, C. J. *Adv. Mater.* **2006**, *18*, 789–794.
- (47) He, Y. J.; Zhao, G. J.; Peng, B.; Li, Y. F. *Adv. Funct. Mater.* **2010**, *20*, 3383–3389.
- (48) Malliaras, G. G.; Salem, J. R.; Brock, P. J.; Scott, C. *Phys. Rev. B* **1998**, *58*, 13411–13414.
- (49) Goh, C.; Kline, R. J.; McGehee, M. D.; Kadnikova, E. N.; Frechet, J. M. J. *Appl. Phys. Lett.* **2005**, *86*, 12110.
- (50) Blom, P. W. M.; Mihailitchi, V. D.; Koster, L. J. A.; Markov, D. E. *Adv. Mater.* **2007**, *19*, 1551–1566.
- (51) Hoppe, H.; Sariciftci, N. S. *J. Mater. Chem.* **2006**, *16*, 45–61.
- (52) Moule, A. J.; Meerholz, K. *Adv. Funct. Mater.* **2009**, *19*, 3028–3036.
- (53) Chen, L. M.; Hong, Z.; Li, G.; Yang, Y. *Adv. Mater.* **2009**, *21*, 1434–1449.
- (54) Mondal, R.; Ko, S.; Verploegen, E.; Becerril, H. A.; Toney, M. F.; Bao, Z. *J. Mater. Chem.* **2010**, *20*, DOI: 10.1039/C0JM02491K.